A Computational Study of the Reaction of Ground-State Nitrogen Atoms with Chloromethyl Radicals

Alvaro Cimas,[†,‡] Víctor M. Rayón,[†] Massimiliano Aschi,[‡] Carmen Barrientos,[†] José A. Sordo,[§] and Antonio Largo*[,†]

Departamento de Química Física, Facultad de Ciencias, Universidad de Valladolid, 47005 Valladolid, Spain, Dipartimento di Chimica, Ingegneria Chimica e Materiali, Universitá di L'Aquila, Via Vetoio (Coppito 2), I-67010 L'Aquila, Italy, and Laboratorio de Química Computacional, Departamento de Química Física y Analítica, Facultad de Química, Universidad de Oviedo, 33006, Oviedo, Spain

Received: February 16, 2005; In Final Form: June 2, 2005

A computational study of the $N(^4S) + CH_2Cl$ reaction has been carried out. The first step of the reaction is the formation of an initial intermediate (NCH_2Cl), which is relatively stable and does not involve any energy barrier. The two most exothermic products are those resulting from the release of a chlorine atom, $H_2C{=}N + Cl$ and *trans*-HC═NH + Cl. A kinetic study within the framework of the statistical theories suggests that the kinetically preferred product is also the most exothermic one. This is in contrast with the analogue reaction of nitrogen atoms with CH_2F, where the preferred product from both thermodynamic and kinetic points of view is HFCN + H. Therefore, reactions of nitrogen atoms with chloromethyl radicals release chlorine atoms as major products. The rate coefficient for the title reaction is estimated to be about 3.09×10^{-13} cm^3 s^{-1} molecule^{-1} at 300 K, a value four times smaller than the rate coefficient for its fluorine analogue.

Introduction

Atom-radical reactions are very important in atmospheric chemistry,[1,2] and in addition, their mechanistic implications are relevant from the general perspective of gas-phase chemistry. Because of its relevance in both atmospheric and combustion chemistry the reactions of oxygen atoms with different radicals have received considerable attention. In particular, the reactions with halogenated alkyl radicals are very interesting because of their implications in atmospheric chemistry. This fact has motivated a number of studies for the reactions of oxygen atoms with simple halogenated alkyl radicals from both the experimental[3−6] and theoretical[7−11] sides.

The reactions of ground-state nitrogen with halogenated alkyl radicals have also received attention. Experimental studies[12−15] have been conducted for reactions of $N(^4S)$ with CHF, CF_2, and CF_3 radicals, and quite recently two theoretical studies[16,17] have addressed the reaction of ground-state nitrogen with CH_2F radicals. Theoretical studies might give rise to interesting predictions. For example, in the computational study of the kinetics of the reaction of $N(^4S)$ with CH_2F[17] it is concluded that, for any value of internal energy and angular momentum, the elimination of a hydrogen atom is always kinetically favored over elimination of a fluorine atom. In addition, theoretical studies provide important information about the possible mechanisms through which these reactions might proceed. In this case, an interesting question is the effect of halogenation in the reactions of nitrogen atoms with alkyl radicals. The reaction of $N(^4S)$ with methyl radicals is interesting due to its astrophysical relevance[18,19] and its importance in combustion processes.[20] Therefore, both experimental[21,22] and theoretical[23,24] studies have been performed for the reaction of ground-state nitrogen and CH_3 radicals.

In the present work a computational study of the reaction of $N(^4S)$ with CH_2Cl is carried out. Different possible channels for this reaction are considered and, to make predictions about the preferred products, a kinetic study within the frame of statistical theories is performed.

Computational Methods

The theoretical methods employed in this work are similar to those used in our previous study of the $N(^4S) + CH_2F$ reaction.[16] The optimizations of geometries and the vibrational frequency calculations were carried out within the framework of both second-order Møller−Plesset (MP2)[25] and the density functional (DFT)[26] theories, employing Dunning's triple-ζ cc-pVTZ basis set.[27] For the DFT calculations we selected the B3LYP level, which is a combination of Becke's 3-parameter exchange functional[28] and the correlation functional of Lee−Yang−Parr.[29] To obtain more accurate energies we have also carried out calculations at both levels, MP2 and B3LYP, with the cc-pVXZ (X = D, T, Q) correlated-consistent basis set in order to estimate complete basis-set (CBS) limits. The CBS extrapolations are based on the important property of Dunning's correlation-consistent basis sets that exhibit monotonic convergence to an apparent complete basis set limit.[30] We used a mixed exponential/Gaussian function of the form

$$E(x) = E_{CBS} + B \exp[-(x-1)] + C \exp[-(x-1)^2] \quad (1)$$

where $x = 2$ (DZ), 3 (TZ), or 4 (QZ), and B and C are fitting constants. Although several alternate expressions are available, our previous experience[31] showed that no significant differences arise from the different extrapolation models.

In the case of MP2 calculations we employed approximate projected MP2 energies,[32] because spin contamination might

* Corresponding author. E-mail address: alargo@qf.uva.es.
† Universidad de Valladolid.
‡ Universitá di L'Aquila.
§ Universidad de Oviedo.

10.1021/jp0508148 CCC: $30.25
Published on Web 07/01/2005

affect the convergence of the MP series. On the other hand, DFT calculations are virtually free of spin contamination. Furthermore, we have also employed two different higher-levels of theory in order to refine the electronic energy and to compare their performance. G2[33] calculations were carried out, thus electronic energies are computed (making additivity assumptions) at the QCISD(T)/6-311+G(3df,2p) level, where QCISD(T) means quadratic configuration interaction with single and double excitations followed by a perturbative treatment of triple excitations. The G2 calculations were performed according to the standard procedure,[33] with the only exception of the use of projected-MP energies instead of unprojected ones. Finally, for the B3LYP geometries, we carried out coupled cluster calculations,[34] CCSD(T)/cc-pVTZ, which constitutes a single and double excitations model augmented with a noniterative triple excitation correction. The intrinsic reaction coordinate (IRC) method[35,36] was employed to connect the different minima located on the potential energy surface (PES). The quantum chemical calculations were performed with the GAUSSIAN 98 package of programs.[37]

Kinetic calculations have been carried out within the framework of the statistical kinetic theories. Even though such an approach has well-known limitations,[38] in practice it is the only tool for study at a semiquatitative level of complicated reactions such as the present one. For the formation of the initial intermediate, as well as for those processes where no transition structure was found (i.e., direct dissociations), we adopted the microcanonical variational transition state theory (μVTST) in its vibrator formulation.[39,40] In this connection, the potential energy paths of the above processes were first scanned. Subsequently, for each point of the scan, the Hessian matrices, describing the modes orthogonal to the reaction path, were evaluated according to the standard procedure of Miller.[41,42]

For the unimolecular reactions involving all the intermediates, the microcanonical rate coefficients have been calculated employing the usual equation of RRKM theory (eq 2).[43]

$$k(E,J) = \sigma N^{\#}(E,J)/[h\rho(E,J)] \qquad (2)$$

where σ is the reaction symmetry factor, $N^{\#}(E,J)$ and $\rho(E,J)$ are, respectively, the number of states at the transition state and the density of states at the minimum evaluated for an energy E and a total angular momentum J.

The determination of the density and sum of states was carried out with the Forst algorithm[44] using the corresponding frequencies and moments of inertia. All required data for intermediates and transition states are provided in Tables S1 and S2, respectively, of the Supporting Information. The possibility of tunneling was accounted for in terms of a monodimensional probability according to the generalized Eckart potential.[45] Finally, thermal rate coefficients were evaluated by averaging over the Boltzmann distribution. All the kinetic calculations were carried out with our own routines, employing the CCSD(T)/cc-pVTZ//B3LYP/cc-pVTZ energies and B3LYP/cc-pVTZ geometries and vibrational frequencies. In our previous study on the N(^{4}S) + CH_2F reaction,[16] we employed the B3LYP/CBS//B3LYP/cc-pVTZ energies. We have preferred to employ in the present case CCSD(T)/cc-pVTZ//B3LYP/cc-pVTZ energies, because in principle they should be more reliable.

Results and Discussion

The most significant geometrical parameters for the reactants and products of the title reaction are shown in Figure 1. We have considered the formation of both primary products resulting from elimination of either hydrogen or chlorine atoms (H_2C=N + Cl, HC=NH + Cl, HClC=N + H, ClC=NH + H, and CNH_2 + Cl) as well as secondary products resulting from further evolution of the primary formed species (HC≡N +H + Cl, and ClC≡N + H + H). The geometries for the intermediates and transition structures located on the [NCH_2-Cl] triplet surface are collected in Figure 2 and Figure 3, respectively. We have checked that intermediates as well as reactants and products correspond to local minima with all real vibrational frequencies, whereas transition structures exhibit one imaginary frequency corresponding to the desired normal mode. Inspection of the geometrical parameters collected in Figures 1−3 shows that the agreement between the B3LYP and MP2 predicted geometries is, in general, good. It is observed, however, that neither intermediates nor products in which there is an N−Cl bond have been found at the B3LYP level. At the MP2 level we have located the product HC•=NCl (see Figure 1) and the intermediates $H_2C^{\bullet}ClN^{\bullet}$ (**I0**) and $H_2C^{\bullet}N^{\bullet}Cl$ (**I4**, see Figure 2 and discussion below). To provide information about the electronic structure of the different species involved in the reaction, we will represent, whenever possible, "limiting structures" obtained from the spin density analysis. Thus, for

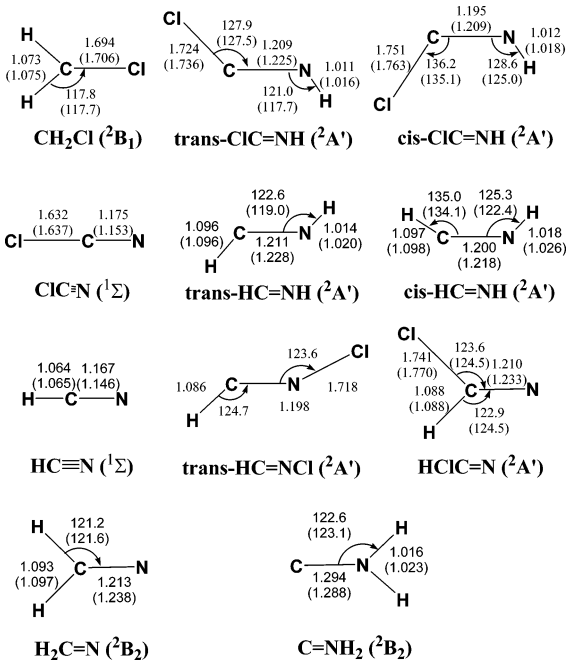

Figure 1. Geometrical parameters as computed at the MP2/cc-pVTZ and B3LYP/cc-pVTZ (in parentheses) levels for the reactant and possible products of the reaction N(^{4}S) + CH_2Cl. Bond distances are given in angstroms and angles in degrees.

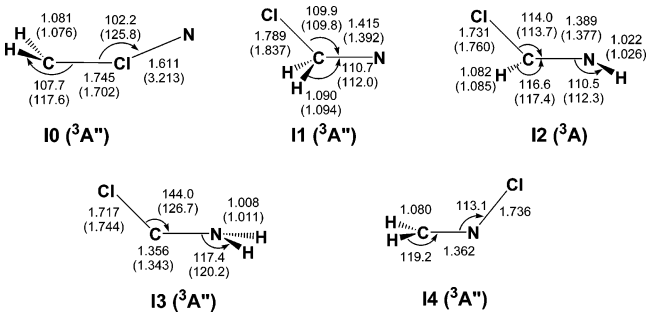

Figure 2. Geometrical parameters as computed at the MP2/cc-pVTZ and B3LYP/cc-pVTZ (in parentheses) levels for the intermediates in the reaction of N(^{4}S) + CH_2Cl. Bond distances are given in angstroms and angles in degrees.

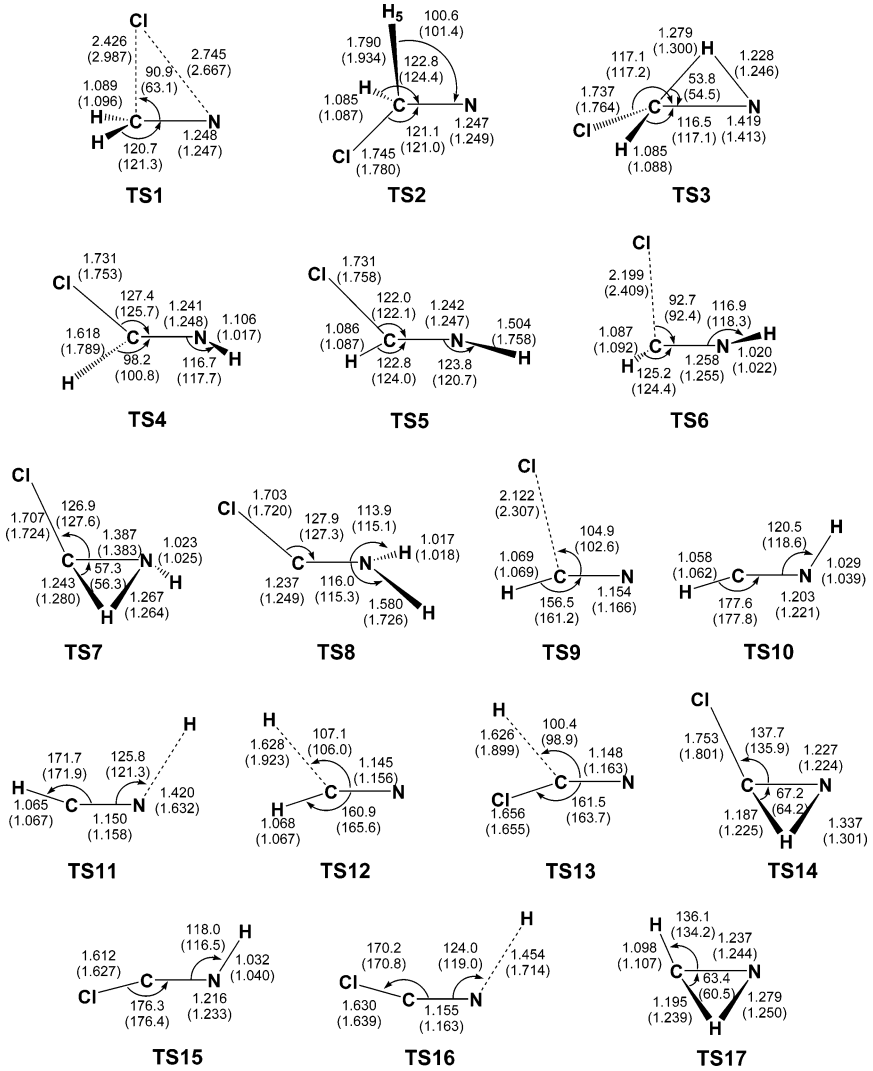

Figure 3. Geometrical parameters as computed at the MP2/cc-pVTZ and B3LYP/cc-pVTZ (in parentheses) levels for the transition structures in the reaction of $N(^4S) + CH_2Cl$. Bond distances are given in angstroms and angles in degrees.

example, $H_2C^{\bullet}ClN^{\bullet}$ represents a structure with pronounced diradical character "mainly" ascribed to the carbon and nitrogen atoms.

The energetic profile for the reaction up to formation of the primary products, as computed at the CCSD(T)/cc-pVTZ and G2 levels, is presented in Figure 4. Figure 5 shows the possible processes that yield the secondary products, obtained through a second elimination of either hydrogen or chlorine.

The relative energies of products, intermediates and transition structures with respect to the reactants $CH_2Cl(^2B_1) + N(^4S)$ are collected in Table 1. Inspection of these data shows that the CCSD(T)/cc-pVTZ method systematically provides energies which are 4−6 kcal/mol lower than the G2 values. It has been noticed elsewhere,[46] and also in our previous paper on the reaction $CH_2F(^2A') + N(^4S)$,[16] that, if the relative energies are computed with respect to one of the intermediates, the CCSD-(T) values get closer to the G2 ones. We concluded then[16] that the discrepancy between the CCSD(T) and G2 energies is related, at least in part, to the description of $N(^4S)$. More specifically, the G2 method includes a higher-level empirical correction (HLC) which seems to be important for the description of $N(^4S)$. Interestingly, the MP2/CBS relative energies are closer to the G2 ones than the CCSD(T) values. This result is consistent with the fact that both methods, MP2/CBS and G2, do include corrections for basis set effects. In fact, we have checked that the MP2/cc-pVTZ relative energies are very close to the CCSD(T)/cc-pVTZ ones. This result also suggests that the correlation contributions are reasonably well estimated already at the MP2 level. In conclusion, we ascribe the discrepancies in the relative energies provided by CCSD(T), when compared to those obtained with the G2 method, to both the lack of the high-level empirical correction (HLC), apparently important for a correct description of $N(^4S)$, and the basis set used in the CCSD(T) calculations (for which a value of 4 kcal/mol from the CBS limit is obtained). Finally, it is also observed that the B3LYP relative energies are, in general, overestimated (relative to the G2 values) by around 5−6 kcal/mol. Inspection of the results collected in Table 1 shows that the general trend in the relative energies is ΔH_0(CCSD(T)/cc-pVTZ) < ΔH_0(G2) ≈ ΔH_0(MP2/CBS) < ΔH_0(B3LYP/CBS).

A brief comment on S^2 expectation values is also in order. For most of the triplet species the S^2 expectation values exceed the spin-pure value by less than 10%. The only exceptions are **TS1** and **TS2**, with $\langle S^2 \rangle$ values of 2.230 and 2.259 (HF/cc-pVTZ wave function). There are also only small deviations in most of the doublet species, the worst behavior being observed for some of the transition states shown in Figure 5, which are involved in the further evolution of the primary products (therefore not affecting those species involved in the kinetic calculations; see below). All S^2 expectation values, along with

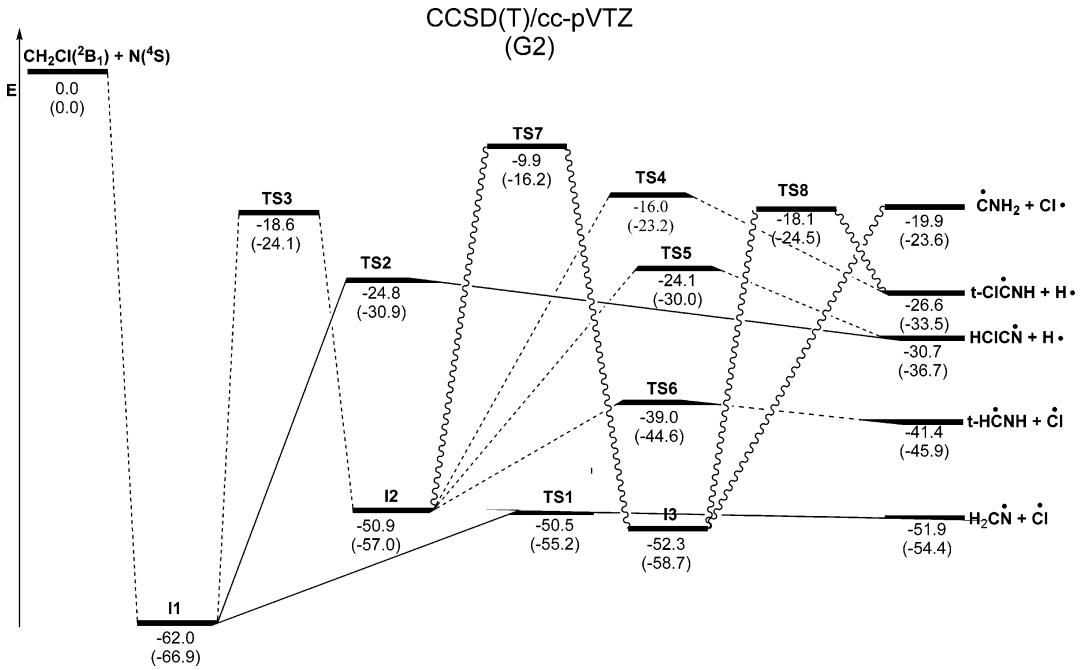

Figure 4. Reaction profile (kcal/mol) at the CCSD(T)/cc-pVTZ and G2 (in parentheses) levels for the formation of the primary products resulting from elimination of either hydrogen or chlorine atoms in the reaction $N(^4S) + CH_2Cl$.

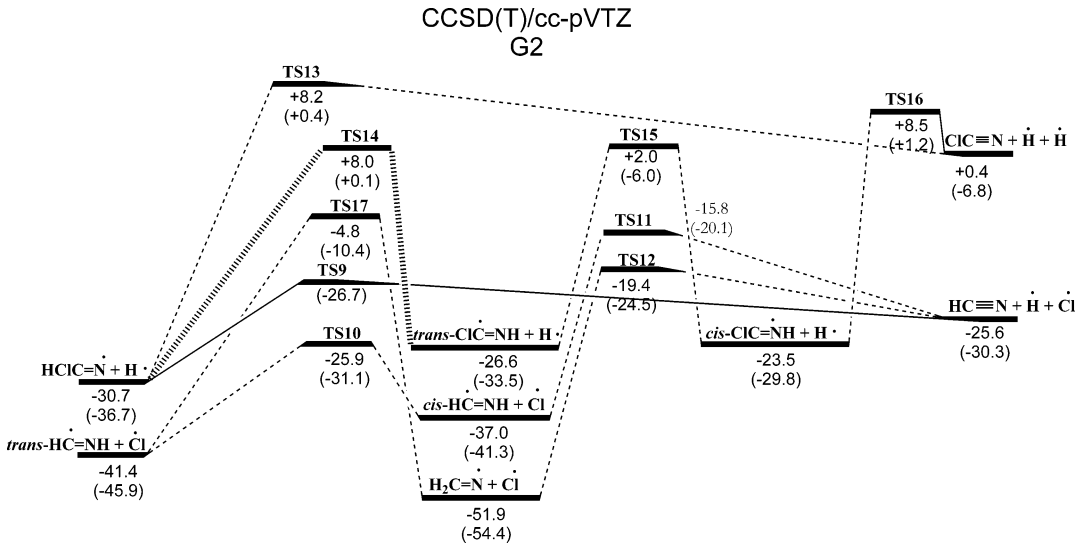

Figure 5. Reaction profile (kcal/mol) at the CCSD(T)/cc-pVTZ and G2 (in parentheses) levels for the possible further evolution of the primary products.

the G2 and CCSD(T) molecular energies, are given as Supporting Information (Table S3).

Before proceeding with the analysis of the results obtained in this study, a short comment should be made about the geometry of the reactant CH_2Cl. In agreement with experimental results,[47,48] CH_2Cl is predicted to be planar at the B3LYP/cc-pVTZ level. At the MP2 level, however, the planar structure shows one imaginary frequency, with a true minimum having been located on a C_s PES. In any case, the deviation from planarity is small (the dihedral angle HCClH is 183°). We will therefore assume that the electronic state of this species is $^2B_1$, with C_{2v} symmetry.

[NCH_2Cl] Triplet PES

The approach of $N(^4S)$ atoms to $CH_2Cl(^2B_1)$ results in two possible intermediates depending on whether the reactants approach toward the chlorine (intermediate **I0**) or the carbon atom (intermediate **I1**, see Figure 2). At the B3LYP level, **I0** ($^3A''$) is a weakly bound molecule $H_2C^{\bullet}Cl\cdots N$ with a Cl···N distance of 3.213 Å. The spin density analysis shows that, as expected, nitrogen and carbon conserve their unpaired electrons. We have checked that, at this level of theory, approaching of the reactants at shorter distances takes place along a repulsive surface. At the MP2/cc-pVTZ level, on the contrary, **I0** ($^3A''$) is a true covalent molecule with a Cl−N bond distance of 1.611 Å. This intermediate is, in fact, a diradical that can be schematically represented as $H_2{}^{\bullet}CClN^{\bullet}$, lying clearly above the reactants, with $\Delta H_0 = +34.4$ kcal/mol (see Table 1). At the MP2/cc-pVDZ level we found a geometrically similar intermediate **I0** but with a different electronic distribution in which the two unpaired electrons are located on the nitrogen atom, $H_2CClN^{\bullet\bullet}$. No intermediate **I0** with a net spin density of −2 on

TABLE 1: Relative Energies (in kcal/mol) at Different Levels of Theory for the Different Species Involved in the Reaction of N (^{4}S) with CH_2Cl ($^2B_1$)

system	MP2/CBS[a]	G2	B3LYP/CBS[b]	CCSD(T)[b]
$CH_2Cl(^2B_1) + N(^4S)$	0.0	0.0	0.0	0.0
trans-ClC•═NH + H•	−38.5	−33.5	−37.4	−26.6
cis-ClC•═NH + H•	−35.6	−29.8	−34.5	−23.5
ClC≡N + H• + H•	−17.5	−6.8	−3.9	0.4
trans-HC•═NH + Cl•	−45.5	−45.9	−51.8	−41.4
cis-HC•═NH + Cl•	−41.1	−41.3	−47.9	−37.0
HC≡N + H• + Cl•	−36.1	−30.3	−29.8	−25.6
trans-HC•═NCl + H•	−6.7	−3.6		
HClC═N• + H•	−37.7	−36.7	−39.9	−30.7
H_2C═N• + Cl•	−50.2	−54.4	−59.7	−51.9
•C═NH2($^2B_2$) + Cl•	−22.4	−23.6	−29.6	−19.9
I0	+34.4[c]	+18.5	+0.2	+0.4
I1	−66.4	−66.9	−70.9	−62.0
I2	−58.0	−57.0	−63.8	−50.9
I3	−62.7	−58.7	−65.2	−52.3
I4	−43.2	−45.8		
TS1	−52.1	−55.2	−62.1	−50.5
TS2	−30.8	−30.9	−35.7	−24.8
TS3	−25.2	−24.1	−29.7	−18.6
TS4	−23.7	−23.2	−29.3	−16.0
TS5	−27.6	−30.0	−36.1	−24.1
TS6	−43.4	−44.6	−52.8	−39.0
TS7	−19.7	−16.2	−22.9	−9.9
TS8	−26.1	−24.5	−31.8	−18.1
TS9	−29.2	−26.7		
TS10	−30.8	−31.1	−38.2	−25.9
TS11	−20.8	−20.1	−24.8	−15.8
TS12	−24.0	−24.5	−26.3	−19.4
TS13	−3.6	+0.4	+1.4	+8.2
TS14	−5.0	+0.1	−1.4	+8.0
TS15	−11.0	−6.0	−11.4	+2.0
TS16	−4.0	+1.2	+0.1	+8.5
TS17	−10.8	−10.4	−13.9	−4.8

[a] IncludingZPE at the MP2/cc-pVTZ level. [b] IncludingZPE at the B3LYP/cc-pVTZ level. [c] MP2/cc-pVTZ+ZPE(MP2/cc-pVTZ) value; see the text.

nitrogen was found on the MP2/cc-pVTZ surface (and for this reason it was not possible to compute the MP2/CBS energies for these two species). Fortunately, G2 calculations could be performed on both intermediates; the results show that both of them lie quite above the reactants, with $\Delta H_0 = +18.5$ kcal/mol (H_2•CClN•) and +24.3 kcal/mol (H_2CClN••). We would finally like to point out that we have also explored the possibility of an intermediate with a $^3A'$ electronic state, but all the optimizations ended up in one of the two $^3A''$ structures.

We can therefore conclude that the approach toward the chlorine atom definitely takes place along a repulsive potential energy surface. Hence, the reaction $N(^4S) + CH_2Cl(^2B_1)$ starts through the interaction of the nitrogen and carbon atoms, intermediate **I1**, a process that takes place directly without involving any transition state. To check that this is in fact the case we have performed scans of the B3LYP and MP2 potential energy surfaces, with the reactants at different C−N distances and optimizing all other geometrical parameters. The results clearly show that the reactants interact on an attractive potential surface. Intermediate **I1** is a rather stable molecule, which lies 62.0 kcal/mol below the reactants (at the CCSD(T) level; from now on, the CCSD(T)/cc-pVTZ//B3LYP/cc-pVTZ energies will be used unless otherwise stated).

Once the intermediate **I1** is formed, several possibilities are opened. **I1** can release a chlorine atom to give the primary product H_2C═N• + Cl•, which is the most exothermic among the possible products of the reaction (−51.9 kcal/mol). Elimination of the chlorine atom involves a barrier of 11.5 kcal/mol (**TS1**). At the B3LYP/cc-pVTZ level of theory, **TS1** does not yield directly H_2C═N• + Cl•, but a weakly bound complex ($\Delta H_0 = -0.3$ kcal/mol, relative to the products), that can be represented as H_2C═N•···Cl•. Because of the large internal energy of this complex, it should quickly release the loosely bonded chlorine atom. For this reason, we have neither included this weakly bound complex in Figure 4 nor considered it for the kinetic calculations (vide infra). At the G2 level of theory, **TS1** becomes slightly lower in energy than H_2C═N• + Cl• (see Figure 4 and Table 1. Note that, at the MP2/cc-pVTZ unprojected level, it lies above the products). This suggests that the elimination of chlorine atoms from the intermediate **I1** is in fact a direct process.

I1 may also evolve through hydrogen elimination (**TS2**; 37.2 kcal/mol relative to **I1**) to yield the products HClC═N• + H• which lie −30.7 kcal/mol below the reactants.

Finally, a hydrogen atom can migrate in **I1** from the carbon to the nitrogen atom to yield the intermediate HClC•N•H, **I2** (−50.9 kcal/mol). This process involves a high barrier (**TS3**, 43.4 kcal/mol), but it is still lower in energy than the reactants (−18.6 kcal/mol).

I2 may further evolve in four different ways: two hydrogen eliminations (from the carbon atom, **TS4**, and from the nitrogen atom, **TS5**), a chlorine elimination (**TS6**) and a second hydrogen migration from carbon to nitrogen (**TS7**), a process that leads to the intermediate ClC••NH_2, **I3** (−52.3 kcal/mol), the second most stable species on the triplet PES. The two hydrogen elimination paths from **I2** involve relatively high barriers, 34.9 kcal/mol (**TS4**) and 26.8 kcal/mol (**TS5**). For the elimination of chlorine, however, a barrier of only 11.9 kcal/mol, which is almost the energy difference between intermediate **I2** and the products *trans*-HC•═NH + Cl•, must be overcome. Finally, hydrogen migration from carbon to nitrogen yields **I3** from **I2**. This process involves a high barrier of 41.0 kcal/mol.

Intermediate **I3** can then either undergo hydrogen elimination through **TS8** (with a barrier height of 34.2 kca/mol) or release a chlorine atom through a direct process to give •CNH_2 + Cl•.

The two most exothermic primary products of this reaction are those in which a chlorine atom is released: H_2C═N• + Cl• (−51.9 kcal/mol) and *trans*-HC•═NH + Cl• (−41.4 kcal/mol). This is at variance with what was found for the CH_2F ($^2A'$) + $N(^4S)$ reaction where the most exothermic products were those that release a hydrogen atom HFC═N• + H• and *trans*-FC•═NH + H•.[16] Interestingly, the exothermicity of these two products with respect to the reactants does not change much when fluorine is substituted by chlorine: HFC═N• + H• (−34.3 kcal/mol) vs HClC═N• + H• (−30.7 kcal/mol), and *trans*-FC•═NH + H• (−31.0 kcal/mol) vs *trans*-ClC•═NH + H• (−26.6 kcal/mol). Instead, those products which involve halogen elimination (H_2CN• + X• and *trans*-HC•NH + X•; X = F, Cl) are about 25 kcal/mol more exothermic when the halogen is chlorine. This is obviously due to the tighter binding of fluorine to carbon. For example, the halogen exchange reaction, $CH_2Cl + F \rightarrow CH_2F + Cl$, has an electronic reaction energy of $\Delta H_0 = -25.9$ kcal/mol at the G2 level of theory, a value that virtually matches the energy difference between the halogen-releasing products of the title reaction.

We have not considered the possible formation of the products HC≡N + HCl and ClC≡N + H_2 since one of the molecules must be in the triplet state, thus giving rise to rather endothermic channels. On the other hand, no path leading to HC•═NCl + H• has been presented in Table 1 and Figure 4 (Note that the species with a N−Cl covalent bond have only been located in the MP2 potential energy surfaces). This is due to two main

reasons. First, the product *trans*-HC•═NCl+ H• is slightly exothermic (−3.6 kcal/mol at the G2 level) and, second, we have not found a path that leads to the precursor of this product (**I4**, see Figure 2) from the initial intermediate **I1**. The only process that would yield **I4** seems to be the recombination of the primary products $H_2C{=}N^\bullet + Cl^\bullet$ through an approach of the chlorine atom to the nitrogen.

From the kinetic point of view, formation of $H_2C{=}N^\bullet + Cl^\bullet$ should also be the most favored process for it involves no barrier at all. We will discuss in more detail the kinetics of this reaction below.

Once the primary products are formed we have considered the formation of secondary products through elimination of a second hydrogen or chlorine atom. We think, however, that formation of secondary products should not be an important process because a large part of the internal energy of the primary products should have already been removed by the released chlorine and hydrogen atoms before further eliminations could take place. In any case, the only feasible process from the thermodynamic point of view seems to be formation of $HC{\equiv}N + H^\bullet + Cl^\bullet$ (which lies −25.6 kcal/mol below reactants) since the other possible product, $ClC{\equiv}N + H^\bullet + H^\bullet$ is almost isoenergetic with the reactants (−6.8 kcal/mol at the G2 level, +0.4 kcal/mol at the CCSD(T) level).

Formation of $HC{\equiv}N + H^\bullet + Cl^\bullet$ can take place from the primary products HClC═N•, *trans*-HC•═NH, and $H_2C{=}N^\bullet$. Elimination of chlorine from HClC═N• involves, at the G2 level, a transition structure (**TS9**) that lies only 3.6 kcal/mol above the products $HC{\equiv}N + H^\bullet + Cl^\bullet$. At the B3LYP level, on the other hand, we have found that elimination of chlorine is a direct process. We therefore think that the activation energy required for the elimination of chlorine from HClC═N• will be on the order of 5.1 kcal/mol, which is the value for the endothermic process. Isomerization of *trans*-HC•═NH into *cis*-HC•═NH (which is about 5 kcal/mol less stable than the trans isomer) followed by hydrogen elimination from the nitrogen atom produces again HC≡N. These two processes are subject to relatively high barriers: 15.5 kcal/mol (**TS10**) and 21.2 kcal/mol (**TS11**), respectively. Finally, fragmentation of a hydrogen atom from $H_2C{=}N^\bullet$ requires that a considerable barrier of 32.5 kcal/mol (**TS12**), must be overcome.

Formation of $ClC{\equiv}N + H^\bullet + H^\bullet$ from the primary product HClC═N• does not seem to be a feasible process from the thermodynamic point of view, as commented above. Figure 5 shows that it also involves high barriers: elimination of hydrogen from the carbon atom requires about 39 kcal/mol (**TS13**) whereas isomerization of HClC═N• into *cis*-ClC•═NH followed by hydrogen elimination is subject to a barrier height of 32.0 kcal/mol.

Our main conclusion from Figure 5 is that further evolution of the primarily formed species is quite unlikely from both the thermodynamic and the kinetic point of view.

We may now compare our results for the title reaction with those obtained for the reaction of nitrogen atoms with CH_2F.[16] In both cases, the analysis of the PESs predicts an addition−elimination mechanism which proceeds through the intermediate $XCH_2N^{\bullet\bullet}$ (**I1**). This intermediate, which lies about 62−65 kcal/mol below the reactants, can further undergo either hydrogen/chlorine elimination or hydrogen isomerization through transition structures which clearly lie below the reactants. Among the primarily formed products, those which release chlorine atoms are, from the thermodynamic point of view, the most favored ones in the [NCH_2Cl] triplet PES. More specifically, we predict the most exothermic product, $H_2CN^\bullet + Cl^\bullet$, to be the preferred one as no activation barrier apart from the endothermicity of the chlorine elimination process is involved. At variance with these results, in the [NCH_2F] triplet PES there was a clear preference for the product HFC═N•, which incorporates a fluorine atom.

Kinetic Calculations

On the basis of the PES determined for the [NCH_2Cl] system we have developed a mechanistic model for the reaction of $N(^4S)$ with chloromethyl radicals. This mechanistic model is depicted in Scheme 1 and it includes basically all the primary products resulting from elimination of either chlorine or hydrogen atoms from the different intermediates **I1**, **I2**, and **I3**. These channels include without any doubt the most relevant ones for the title reaction, and are denoted in order of decreasing exothermicity as follows: **a** ($H_2CN + Cl$); **b** (*trans*-HCNH + Cl); **c** (HClCN + H); **d** (*trans*-ClCNH + H); **e** ($H_2NC + Cl$).

The steady-state solution of the master equation leads to the following microcanonical expression for the overall rate coefficient:

$$k_{\text{overall}}(T) = k_a(T) + k_b(T) + k_c(T) + k_d(T) + k_e(T) \quad (3)$$

where the individual coefficients for the different channels are given by the following formulas:

$$k_a(T) = \frac{1}{hQ_r(T)}\sum_J (2J+1)\int_o^\infty \frac{N_{\text{capt}}(E,J)k_{1a}(E,J)}{B(E,J)} \exp\left(-\frac{E}{kT}\right) dE \quad (4)$$

$$k_b(T) = \frac{1}{hQ_r(T)}\sum_J (2J+1)\int_0^\infty \frac{N_{\text{capt}}(E,J)k_{12}(E,J)k_{2b}(E,J)}{A(E,J)B(E,J)} \exp\left(-\frac{E}{kT}\right) dE \quad (5)$$

$$k_c(T) = \frac{1}{hQ_r(T)}\sum_J (2J+1)\int_0^\infty \frac{N_{\text{capt}}(E,J)}{B(E,J)}\left\{k_{1c}(E,J) + \frac{k_{12}(E,J)k_{2c}(E,J)}{A(E,J)}\right\} \exp\left(-\frac{E}{kT}\right) dE \quad (6)$$

$$k_d(T) = \frac{1}{hQ_r(T)}\sum_J (2J+1)\int_0^\infty \frac{N_{\text{capt}}(E,J)k_{12}(E,J)}{A(E,J)B(E,J)}\left\{k_{2d}(E,J) + \frac{k_{23}(E,J)k_{3d}(E,J)}{k_{-23}(E,J) + k_{3d}(E,J) + k_{3e}(E,J)}\right\} \exp\left(-\frac{E}{kT}\right) dE \quad (7)$$

$$k_e(T) = \frac{1}{hQ_r(T)}\sum_J (2J+1)\int_0^\infty \frac{N_{\text{capt}}(E,J)k_{12}(E,J)k_{23}(E,J)k_{3e}(E,J)}{A(E,J)B(E,J)[k_{-23}(E,J) + k_{3d}(E,J) + k_{3e}(E,J)]} \exp\left(-\frac{E}{kT}\right) dE \quad (8)$$

where $N_{\text{capt}}(E,J)$ is the number of the states evaluated in the barrier free process as described in the methodological section, $Q_r(T)$ are the reactants relative translational partition function

SCHEME 1: Mechanistic Model for the Kinetic Study Employed in the Present Work[a]

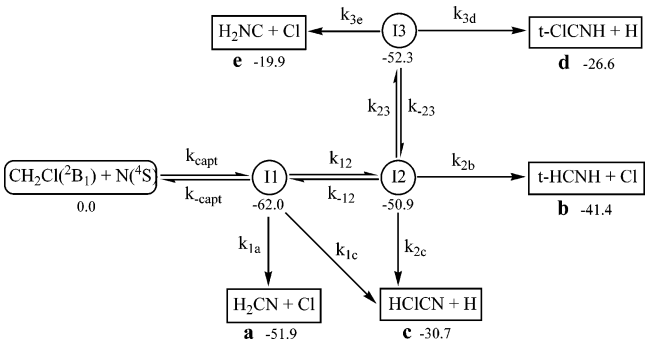

[a] Relative energies at 0 K are in kcal/mol and were computed at the CCSD(T)/cc-pVTZ level, including B3LYP/cc-pVTZ ZPVEs.

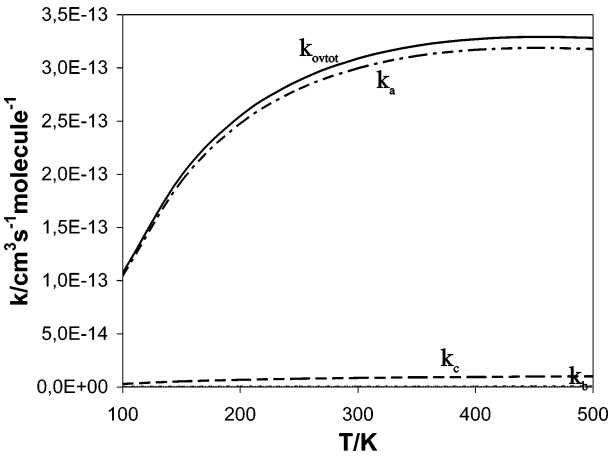

Figure 6. Overall and individual canonical rate coefficients (cm^{-3} s^{-1} $molecule^{-1}$) plotted vs temperature.

at the temperature T and $A(E,J)$ and $B(E,J)$ were calculated according to the following relationships:

$$A(E,J) = k_{-12}(E,J) + k_{23}(E,J) + k_{2b}(E,J) + k_{2c}(E,J) + k_{2d}(E,J) - \frac{k_{23}(E,J)k_{-23}(E,J)}{k_{-23}(E,J) + k_{3d}(E,J) + k_{3e}(E,J)} \quad (9)$$

$$B(E,J) = k_{-capt}(E,J) + k_{12}(E,J) + k_{1a}(E,J) + k_{1c}(E,J) - \frac{k_{12}(E,J)k_{-12}(E,J)}{A(E,J)} \quad (10)$$

Note that each of the above individual rate coefficients, k_i, was evaluated at fixed internal energy and angular momentum J, and therefore, in order to obtain the final canonical rate coefficients, the above expressions were thermally averaged according to a Boltzmann distribution.

The overall and individual canonical rate coefficients are represented in Figure 6 as functions of the temperature. In the cases of channels **d** and **e**, the individual rate coefficients are much smaller than the other ones and are not represented in Figure 6, since they superpose with the abscissa. In all cases the logarithmic representations against $1/T$ show typical linear behavior, and small deviations from linearity are only observed at high temperatures. In the lack of any potential energy barrier, the estimated activation free energy for the overall process is 0.12 kcal/mol a value which is plausibly dominated by entropic activation effects typical of bimolecular reactions. The computed rate coefficient for the overall process at 300 K is 3.09×10^{-13} cm^3 s^{-1} $molecule^{-1}$, a value somewhat smaller (one-quarter) than the corresponding value for the reaction of nitrogen atoms with fluoromethyl radicals.[17] In the present case, however, it may be rather difficult to justify the validity of the approximations made in the RRKM calculations, embodied in the assumption of an efficient internal energy randomization of all the reaction intermediates. For this reason our calculations, both in the present study and in the previous one involving fluoromethyl, should be considered just at a semiquantitative level. The two reactions can be therefore considered as very efficient processes both proceeding at near collision-efficiency with no kinetically relevant differences.

TABLE 2: Reaction Product Branching Fractions at Different Temperatures

T/K	$H_2CN + Cl$	t-HCNH + Cl	HClCN + H
100	0.9724	0.0012	0.0264
150	0.9722	0.0012	0.0266
200	0.9718	0.0013	0.0269
250	0.9714	0.0013	0.0273
300	0.9708	0.0013	0.0279
350	0.9702	0.0013	0.0285
400	0.9695	0.0014	0.0291
450	0.9688	0.0014	0.0298
500	0.9679	0.0014	0.0307

As it can be seen in Figure 6, channel **a** has the largest individual rate coefficient. In fact, the individual rate coefficients can be qualitatively ordered, according to their magnitudes, as follows: $k_a \gg k_c > k_b \gg k_d \approx k_e$. The corresponding product branching ratios at different temperatures are collected in Table 2. The branching ratios for channels **d** and **e** are not shown in Table 2 since their values are always below 10^{-5}, and consequently they are virtually zero. The most important conclusion is that there is no doubt that the dominant channel (with branching fractions always above 0.96) for the reaction of nitrogen atoms with chloromethyl radicals is channel **a** (that is, $H_2CN + Cl$), which is the most exothermic one. Only residual quantities of HClCN + H and t-HCNH + Cl should be produced. In fact, the results for these two channels show that, under kinetic control, the largest secondary product should be HClCN + H, which is less exothermic than t-HCNH + Cl at all levels of theory.

The results for the individual rate coefficients are consistent with the general overview of the PES for the [NCH_2Cl] system. The dominant channel, $H_2CN + Cl$, involves formation of intermediate **I1** (which does not imply any energy barrier) and elimination of chlorine through **TS1**, which is the lowest-lying transition state and lies only about 12 kcal/mol above **I1**. Channel **c**, production of HClCN + H, proceeds through elimination of a hydrogen atom from **I1** through a transition state lying considerably higher, about 36 kcal/mol above **I1**. There is another alternative path to channel **c**, taking place through **I2**, but the transition state for **I1**-**I2** isomerization lies even higher in energy (about 43 kcal/mol above **I1**). The other secondary channel, leading to *trans*-HCNH + Cl (**b**), necessarily involves isomerization into **I2**, and therefore it is even less competitive than channel **c**. Furthermore, an analysis of the most important unimolecular coefficients shows that there are no significant changes with the internal energy, and therefore under any dynamical condition $H_2CN + Cl$ should be the preferred products.

To make a comparison of the title reaction with the analogue reaction of nitrogen atoms with fluoromethyl radicals,[17] a schematic representation of the two most competitive channels for both processes is depicted in Figure 7. The origin of the main differences between both reactions can be seen clearly in Figure 7. The $H_2CN + X$ channel is much more exothermic in

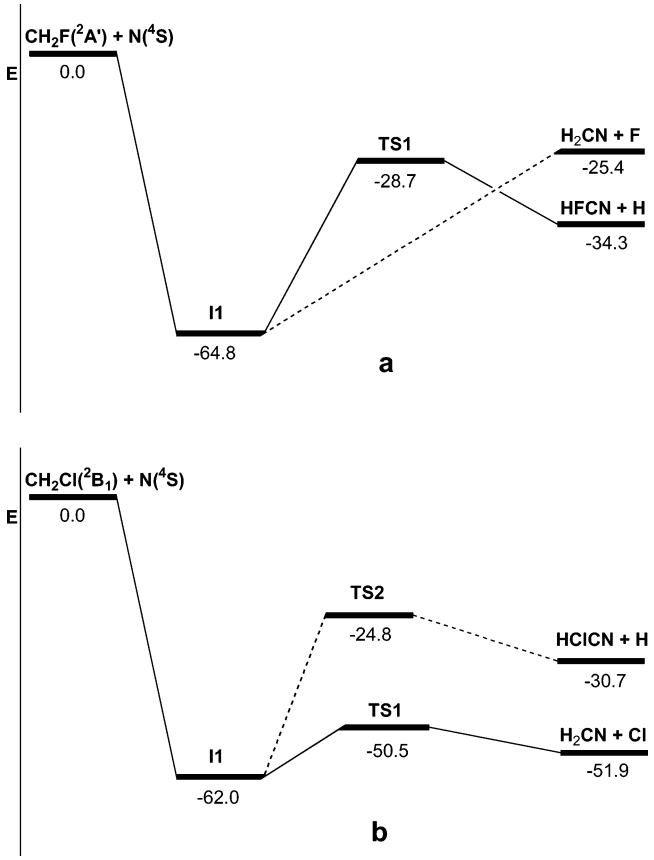

Figure 7. Schematic representation of the two most competitive channels for the reaction $N(^4S) + CH_2F$ (panel a) and $N(^4S) + CH_2Cl$ (panel b). Relative energies (kcal/mol) have been obtained at the CCSD-(T)/cc-pVTZ level including B3LYP/cc-pVTZ ZPE.

the case of chlorine and involves a much lower energy barrier than for fluorine. Furthermore, the difference in the relative energies of transition states **TS1** and **TS2** for chloromethyl radicals is quite high. This is the main reason for the clear predominance of the $H_2CN + Cl$ channel for this reaction. In the case of the reaction with fluoromethyl radicals, even though the $HFCN + H$ channel is more exothermic and involves a lower barrier, the $H_2CN + F$ channel has a relative energy not too far from that of **TS1**. Therefore, even though $HFCN + H$ is the dominant channel, $H_2CN + F$ has a nonnegligible contribution[17] (the predicted branching ratio is nearly 0.25).

Conclusions

A computational study of the reaction of ground-state nitrogen atom with the chloromethyl radical has been carried out. From the analysis of the triplet potential energy surface for the [NCH_2-Cl] system we can conclude that the reaction starts from the interaction of the nitrogen and carbon atoms, leading to the formation of an initial intermediate (NCH_2Cl), which is relatively stable. The formation of this initial intermediate does not involve any energy barrier, and therefore, it is a direct process. The two most exothermic products are those in which a chlorine atom is released: $H_2C{=}N + Cl$ (−51.9 kcal/mol at the CCSD(T)/cc-pVTZ level) and *trans*-$HC{=}NH + Cl$ (−41.4 kcal/mol). Elimination of a hydrogen atom results in less exothermic products: $HClCN + H$ (−30.7 kcal/mol) and *trans*-$ClCNH + H$ (−26.6 kcal/mol). As in the case of the analogue reaction of $N(^4S)$ with CH_2F, further evolution of the primary products, via subsequent elimination of either a hydrogen or an halogen atom, is not likely, since all secondary processes are much less exothermic and involve significant energy barriers.

The kinetic study of the $N(^4S) + CH_2Cl$ reaction within the framework of the statistical theories suggests that the preferred product from the kinetic point of view is also the most exothermic one, namely $H_2C{=}N + Cl$, with branching fractions always greater than 0.96. Only minor fractions of other products, mainly $HClCN + H$ (the third product in stability order), are observed at all temperatures. Therefore, there is an important difference with the analogue reaction of nitrogen atoms with fluoromethyl radicals, since for the latter the preferred product both from the thermodynamic and kinetic points of view is $HFCN + H$, that is, elimination of a hydrogen atom and formation of a product containing a carbon−halogen bond. In the case of the reaction of nitrogen atoms with CH_2Cl, chlorine atoms are released and this might be of relevance in the context of atmospheric chemistry. Moreover it is also estimated that the reaction of $N(^4S)$ with CH_2Cl, as in the case for the $N(^4S) + CH_2F$ reaction, should proceed with a rather high efficiency.

Finally we should point out that in the present study we have not considered the possibility of spin-crossing. We have retained the system in its triplet [NCH_2Cl] surface. The quintet surface would also be spin-conserving starting from the $N(^4S) + CH_2$-Cl reactants, but our preliminary explorations at the MP2 level confirmed that the species found on this surface are much less stable than those obtained on the triplet PES. Furthermore, possible quintet products lie also much higher in energy than their triplet counterparts. For example, $H_2CN(^4A'') + Cl(^2P)$ are found about 90 kcal/mol above the most favorable triplet product, $H_2CN(^2B_2) + Cl(^2P)$, at the CCSD(T) level. Therefore, it seems that quintet channels can hardly compete with the fast processes on the triplet surface under the thermal regime. However, it is conceivable that the formation of products, such as $HCN(^1\Sigma^+) + HCl(^1\Sigma^+)$ or $ClCN(^1\Sigma^+) + H_2(^1\Sigma^+)$, without conservation of spin, could take place if the singlet [NCH_2Cl] surface could be reached through a spin flip. Perhaps, as in the case of the $N + CH_3$ reaction,[24] the nonadiabatic mechanism could play a role at low temperatures. We are currently analyzing the possible role of spin crossing for the title reaction.

Acknowledgment. This research has been supported by the Ministerio de Educación y Ciencia of Spain (Grants CTQ2004-07405 and HI2002-0025) and by the Junta de Castilla y León (Grant VA085/03). A.C. gratefully acknowledges a fellowship from the Junta de Castilla y León. The authors thank Prof. S. Fraga (University of Alberta, Canada) for helpful comments.

Supporting Information Available: Vibrational frequencies and rotational constants for the intermediates (Table S1) and transition states (Table S2) employed in the kinetic calculations and molecular energies at the G2 and CCSD(T) levels, along with the $\langle S^2 \rangle$ values (Table S3). This material is available free of charge via the Internet at http://pubs.acs.org.

References and Notes

(1) Wayne, R. P. *Chemistry of Atmospheres*; Oxford University Press: Oxford, England, 1991.

(2) Finlayson-Pitts, B.; Pitts, J. N. *Chemistry of the Upper and Lower Atmosphere*; Academic Press: San Diego, CA, 1999.

(3) Seetula, J. A.; Slagle, I. R.; Gutman, D.; Senkan, S. M. *Chem. Phys. Lett.* **1996**, *252*, 299.

(4) Seetula, J. A.; Slagle, I. R. *Chem. Phys. Lett.* **1997**, *277*, 381.

(5) Yamamori, Y.; Takahashi, K.; Inomata, T. *J. Phys. Chem. A* **1999**, *103*, 8803.

(6) Stoliarov, S. I.; Bencsura, A.; Shafir, E.; Knyazev, V. D.; Slagle, I. R. *J. Phys. Chem. A* **2001**, *105*, 76.

(7) Wang, B.; Hou, H.; Gu, Y. *J. Phys. Chem. A* **1999**, *103*, 2060.

(8) Wang, B.; Hou, H.; Gu, Y. *J. Phys. Chem. A* **1999**, *103*, 5075.

(9) Hou, H.; Wang, B.; Gu, Y. *J. Phys. Chem. A* **1999**, *103*, 8075.

(10) Wang, B.; Hou, H.; Gu, Y. *Chem. Phys. Lett.* **1999**, *304*, 278.
(11) Wang, B.; Hou, H.; Gu, Y. *Chem. Phys.* **1999**, *247*, 201.
(12) Tsai, C.; Belanger, S. M.; Kim, J. T.; Lord, J. R.; McFadden, D. L. *J. Phys. Chem.* **1989**, *93*, 1916.
(13) Tsai, C.; McFadden, D. L. *J. Phys. Chem.* **1990**, *94*, 3298.
(14) Jeoung, S. C.; Choo, K. Y.; Benson, S. W. *J. Phys. Chem.* **1991**, *95*, 7282.
(15) Kumar, S. V. K.; Sathyamurthy, N.; Manogaran, S.; Mitra, S. K. *Chem. Phys. Lett.* **1994**, *222*, 465.
(16) Menendez, B.; Rayon, V. M.; Sordo, J. A.; Cimas, A.; Barrientos, C.; Largo, A. *J. Phys. Chem. A* **2001**, *105*, 9917.
(17) Cimas, A.; Aschi, M.; Barrientos, C.; Rayon, V. M.; Sordo, J. A.; Largo, A. *Chem. Phys. Lett.* **2003**, *374*, 594.
(18) Nejad, L. A. M.; Millar, T. J. *Mon. Not. R. Astron. Soc.* **1988**, *230*, 79.
(19) Yung, Y. L.; Allen, M.; Pinto, J. P. *Astrophys. J. Suppl. Ser. Phys* **1984**, *55*, 465.
(20) Glarborg, P.; Miller, J. A.; Kee, R. J. *Combust. Flame* **1986**, *65*, 177.
(21) Marston, G.; Nesbitt, F. L.; Nava, D. F.; Payne, W. A.; Stief, L. J. *J. Phys. Chem.* **1989**, *93*, 5769.
(22) Marston, G.; Nesbitt, F. L.; Stief, L. J. *J. Chem. Phys.* **1989**, *91*, 3483.
(23) Gonzalez, C.; Schlegel, H. B. *J. Am. Chem. Soc.* **1992**, *114*, 9118.
(24) Sadygov, R. G.; Yarkony, D. R. *J. Chem. Phys.* **1997**, *107*, 4994.
(25) Hehre, W. J.; Radom, L.; Schleyer, P.v. R.; Pople, J. A. *Ab initio Molecular Orbital Theory*; Wiley: New York, 1986.
(26) Koch, W.; Holthausen, M. C. *A Chemist's Guide to Density Functional Theory*, 2nd ed.; Wiley-VCH: Weinheim, Germany, 2000.
(27) Dunning, T. H., Jr. *J. Chem. Phys.* **1989**, *90*, 1007.
(28) Becke, A. D. *J. Chem. Phys.* **1992**, *97*, 9173.
(29) Lee, C.; Yang, W.; Parr, R. G. *Phys. Rev. B* **1988**, *37*, 785.
(30) Dunning, T. H., Jr. *J. Phys. Chem. A* **2000**, *104*, 9062.
(31) Feller, D.; Sordo, J. A. *J. Chem. Phys.* **2000**, *113*, 485.
(32) Schlegel, H. B. *J. Chem. Phys.* **1986**, *84*, 4530.
(33) Curtiss, L. A.; Raghavachari, K.; Trucks, G. W.; Pople, J. A. *J. Chem. Phys.* **1991**, *94*, 7221.
(34) Bartlett, R. J.; Stanton, J. F. *Reviews in Computational Chemistry*, VCH: New York, 1994; Vol. 5.
(35) Gonzalez, C.; Schlegel, H. B. *J. Chem. Phys.* **1989**, *90*, 2154.
(36) Gonzalez, C.; Schlegel, H. B. *J. Chem. Phys.* **1990**, *94*, 5523.
(37) Frisch, M. J.; Trucks, G. W.; Schlegel, H. B.; Scuseria, G. E.; Robb, M. A.; Cheeseman, J. R.; Zakrzewski, V. G.; Montgomery, J. A., Jr.; Stratmann, R. E.; Burant, J. C.; Dapprich, S.; Millan, J. M.; Daniels, A. D.; Kudin, K. N.; Strain, M. C.; Farkas, O.; Tomasi, J.; Barone, V.; Cossi, M.; Cammi, R.; Mennucci, B.; Pomelly, C.; Adamo, C.; Clifford, S.; Ochterski, J.; Petersson, G. A.; Ayala, P. Y.; Cui, Q.; Morokuma, K.; Malick, D. K.; Rabuck, A. D.; Raghavachari, K.; Foresman, J. B.; Cioslowski, J.; Ortiz, J. V.; Baboul, A. G.; Stefanov, B. B.; Liu, G.; Liashenko, A.; Piskorz, P.; Komaromi, I.; Gomperts, R.; Martin, R. L.; Fox, D. J.; Keith, T.; Al-Laham, M. A.; Peng, C. Y.; Nanayakkara, A.; Gonzalez, C.; Challacombe, M.; Gill, P. M. W.; Johnson, B.; Chen, W.; Wong, M. W.; Andres, J. L.; Head-Gordon, M.; Replogle, E. S.; Pople, J. A. *Gaussian 98*. Gaussian Inc.: Pittsburgh, PA, 1998.
(38) Baer, T.; Hase, W. L. *Unimolecular Reaction Dynamics Theory and Experiments*; Oxford University Press: Oxford, England, 1996.
(39) Garrett, B. C.; Truhlar, D. G. *J. Chem. Phys.* **1979**, *70*, 1593.
(40) Hu, X.; Hase, W. L. *J. Chem. Phys.* **1991**, *95*, 8073.
(41) Miller, W. H.; Handy, N. C.; Adams, J. E. *J. Chem. Phys.* **1980**, *72*, 99.
(42) Baboul, A. G.; Schlegel, H. B. *J. Chem. Phys.* **1989**, *90*, 2154.
(43) Robinson, P. J.; Holbrook, K. A. *Unimolecular Reactions*; Wiley: New York, 1972.
(44) Forst, W. *Theory of Unimolecular Reactions*; Academic: New York, 1973.
(45) Miller, W. H. *J. Am. Chem. Soc.* **1979**, *101*, 6810.
(46) Barrientos, C.; Redondo, P.; Largo, A. *J. Phys. Chem. A* **2000**, *104*, 11541.
(47) Endo, Y.; Saito, S.; Hirota, E. *Can J. Phys.* **1984**, *62*, 1347.
(48) Sears, T. J.; Temps, F.; Wagner, H. Gg.; Wolf, M. *J. Mol. Spectrosc.* **1994**, *168*, 136.